Bull. Inst. Chem. Res., Kyoto Univ., Vol. 47, No. 4, 1969

Infrared and Raman Spectra of TCNQ and TCNQ-d_4 Crystals

Tohru TAKENAKA*

Received July 8, 1969

The infrared spectra of the TCNQ and TCNQ-d_4 crystals were observed with polarized radiation incident perpendicularly and obliquely upon the sample plane. From the results obtained, the observed bands were experimentally identified to the three infrared-active species under the assumption of the oriented gas model. The far-infrared spectra and the laser Raman spectra were also obtained for the TCNQ and TCNQ-d_4 samples. An assignment of the observed frequencies to the fundamentals, overtones or combinations was made with the aid of the selection rule, the product rule, the modified sum rule, and comparison of the data with those of the analogous molecules.

1. INTRODUCTION

Fully conjugated cyano-compounds such as tetracyanoethylene (TCNE) and 7, 7, 8, 8-tetracyanoquinodimethane (TCNQ) are well known as representatives of electron acceptors in the charge-transfer complexes to which much attention has been directed. In the previous paper,[1] the present author and Hayashi have studied the infrared and Raman spectra of the TCNE molecule. In the present work, the same type of study has been carried out for the TCNQ and TCNQ-d_4 crystals.

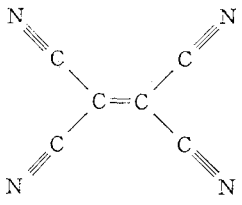

TCNE

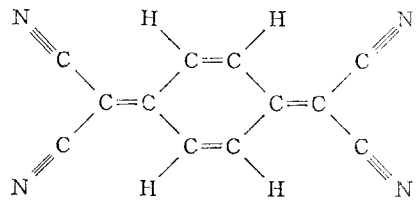

TCNQ

The interpretation of the rather complex spectra of these molecules should be based on the experimental results. For this purpose, the infrared spectra (4000 to 250 cm^{-1}) of the crystals were measured with polarized radiation incident not only perpendicularly but also obliquely upon the sample plane, and the observed vibrations were confidently identified to three symmetry species under the well-known assumption of the oriented gas model.

The far-infrared spectra and the Raman spectra of these samples were also obtained. Comparison of the spectral data with those of partly analogous molecules and application of the product rule[2,3] and the modified sum rule[4] for the

* 竹中　亨 : Laboratory of Surface and Colloid Chemistry, Institute for Chemical Research, Kyoto University, Uji, Kyoto.

TCNQ and TCNQ-d_4 fundamentals offered a great help to the assignment of the observed frequencies to the vibrational modes. The present paper describes the detail of the experimental results and the vibrational assignments obtained.

II. EXPERIMENTAL

A sample of TCNQ was supplied by Dr. N. Uyeda. That of TCNQ-d_4 was synthesized by Dr. S. Oka from 1, 4-cyclohexadione-d_8[5], which was obtained by repetitions of a stepwise reaction between 1, 4-cyclohexadione and heavy water at 170°C for four hours in an autoclave. The completion of the latter reaction was checked by means of the infrared spectrum. Both samples were recystallized three times from acetonitrile solution. The rust-colored, crystalline solids of TCNQ and TCNQ-d_4 thus obtained melt at 291—293° and 295—298°C, respectively, whereas a literature value for the former is 293.5—296°C.[5]

Lozenge shaped, thin single crystals of about 10 mm^2 area were easily grown by the careful recrystallization. The crystal structure of sublimated TCNQ has recently been reported by Long, Sparks and Trueblood[6] to be the monoclinic system, $a=8.906$Å, $b=7.060$Å, $c=16.395$Å and $\beta=98.54°$, Space Group $C2/c—C^6_{2h}$, with four molecules in the unit cell. The Bravais unit cell consists of the half of the crystallographical unit cell, containing two molecules in it. By x-ray diffraction studies, it was found that both the TCNQ and TCNQ-d_4 crystals prepared in the present work had the same crystal form and that the crystal plane developed was the (001) plane *i. e.* the *ab*-plane, keeping the *a*- and *b*-crystal axes parallel to the long and short diagonal lines, respectively, of the sample lozenge.

The polarized infrared spectra of the crystals on normal incidence of radiation were measured between 4000 and 250 cm^{-1} with the aid of a Perkin-Elmer model 521 grating spectrophotometer and a wire grid polarizer. The infrared polarization measurements by the tilting method were carried out from 4000 to 400 cm^{-1} using a Hitachi model EPI-G_3 grating spectrophotometer combined with a Hitachi model IM-K microscope as well as the wire grid polarizer. The far-infrared spectra from 400 to 30 cm^{-1} were obtained in Nujol mulls with the aid of a Hitachi FIS-3 spectrophotometer. The Raman spectra of several lumps of the TCNQ and TCNQ-d_4 crystals were recorded by Dr. M. Ito using a He-Ne gas laser as a light source for excitation (6328Å). In spite of deep color of the crystals, a number of Raman lines were observed. Unfortunately, no line was detected in the region more than *ca* 3000 cm^{-1}, because of low sensitivity of the detector in this region.

III. SELECTION RULES AND CRYSTAL SPECTRA

The TCNQ molecule has essentially $D_{2h}\equiv V_h$ symmetry. Although Long, Sparks, and Trueblood[6] have reported some differences in the bond lengths and angles which are chemically equivalent but not crystallographically equivalent, the differences are apparently so slight that for a discussion of the crystal spectra it can be confidently ignored.

The selection rules for the free molecule and for that in the crystal are shown in the correlation diagram of Table 1. It shows that each vibration of

Table 1. Correlation Diagram and Selection Rules.*

Molecular group $D_{2h}\equiv V_h$	Site group C_i	Factor group C_{2h}
10 A_g (R, p)		
9 B_{1g} (R, dp)	A_g (R)	27 A_g (R, p)
5 B_{2g} (R, dp)		27 B_g (R, dp)
3 B_{3g} (R, dp)		
4 A_u ($i.a.$)		
5 B_{1u} (IR, M_z)	A_u (IR)	27 A_u (IR, M_b)
9 B_{2u} (IR, M_y)		27 B_u (IR, M_{ac})
9 B_{3u} (IR, M_x)		

* R : Raman-active, IR : infrared-active, $i.a.$: inactive,
p : polarized, dp : depolarized.

Table 2. Proportionality Factors for Band Intensity along a, b, and c^* Axes.

Axis	B_{1u}	B_{2u}	B_{3u}
a	0.00	0.56	0.44
b	0.84	0.09	0.07
c^*	0.16	0.35	0.49

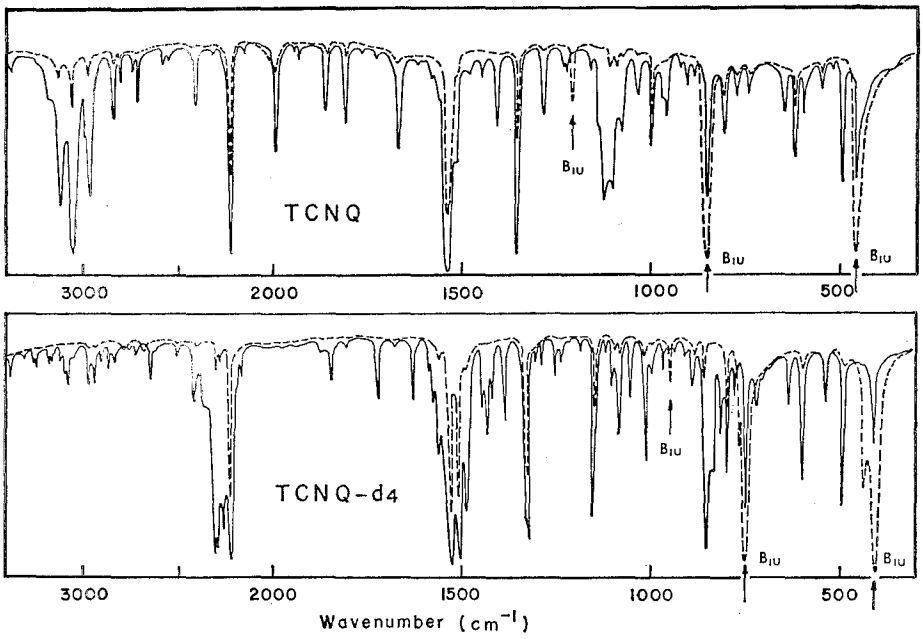

Fig. 1. Polarized infrared spectra of TCNQ (above) and TCNQ-d_4 crystals (below) obtained at normal incidence of radiation on the ab-crystal plane.
——: Electric vector parallel to the a-axis.
– – –: Electric vector parallel to the b-axis.

Table 3. Infrared Spectra of TCNQ and TCNQ-d_4.

TCNQ			TCNQ-d_4		
Frequency (cm^{-1})	Intensity*	Species experimentally determined	Frequency (cm^{-1})	Intensity*	Species experimentally determined
3422	vw	B_{3u}	3422	vw	B_{3u}
3401	vw	B_{3u}	3375	vw	B_{3u}
3330	vw	B_{2u}	3240	vw	B_{2u}
3202	vw	B_{3u}	3228	vw	B_{2u}
3135	m	B_{2u}	3190	vw	B_{2u}
3062	m	B_{3u}	3175	vw	B_{2u}
3048	s	B_{2u}	3155	vw	B_{2u}
2980	sh	B_{2u}	3140	vw	B_{2u}
2970	m	B_{3u}	3075	w	B_{2u}
2848	w	B_{2u}	2965	w	B_{3u}
2805	vw	B_{2u}	2943	w	B_{2u}
2740	vw	B_{3u}	2920	vw	B_{3u}
2710	w	B_{2u}	2865	vw	B_{2u}
2585	vw	B_{2u}	2625	vw	B_{2u}
2555	vw	B_{2u}	2518	vw	B_{3u}
2412	w	B_{2u}	2420	w	B_{2u}
2225	s	B_{2u} and B_{3u}	2375	w	B_{3u}
1995	m	B_{2u}	2295	s	B_{2u}
1922	vw	B_{2u}	2283	s	B_{3u}
1858	m	B_{3u}	2262	m	B_{3u}
1804	m	B_{3u}	2225	s	B_{2u} and B_{3u}
1770	vw	B_{2u}	2175	w	B_{3u}
1718	vw	B_{3u}	1839	w	B_{2u}
1668	m	B_{2u}	1722	m	B_{2u}
1565	sh	B_{2u}	1668	vw	B_{3u}
1543	s	B_{3u}	1628	m	B_{2u}
1537	s	B_{2u}	1582	sh	B_{2u} or B_{3u}
1520	sh	B_{2u}	1555	w	B_{3u}
1475	vw	B_{2u}	1531	s	B_{3u}
1430	vw	B_{2u}	1510	s	B_{2u}
1402	w	B_{3u}	1495	m	B_{2u}
1352	s	B_{2u}	1435	m	B_{3u}
1282	w	B_{2u}	1395	m	B_{2u}
1223	vw	B_{3u}	1318	s	B_{2u}
1214	vw	B_{3u}	1303	vw	B_{2u}
1204	w	B_{1u}	1290	w	B_{3u}
1153	vw	B_{3u}	1249	m	B_{3u}

the free molecule splits in the crystal into two modes, keeping its intrinsic activity unchanged, except for the vibrations in the A_u species of the free molecule which are infrared- and Raman-inactive but their splitting modes (A_u and B_u species) are infrared-active and Raman-inactive. Thus it can be expected that, under a sufficient resolution, each band should be split into two components belonging to

continued

1132	sh	B_{2u}	1234	w	B_{2u}
1122	m	B_{3u}	1181	w	B_{2u} or B_{3u}
1110	m	B_{2u}	1160	s	B_{2u}
1089	m	B_{2u}	1128	w	B_{2u}
1042	w	B_{2u}	1103	w	B_{2u}
996	m	B_{3u}	1090	m	B_{2u}
971	w	B_{2u}	1054	w	B_{2u}
960	m	B_{3u}	1019	m	B_{2u}
915	vw	B_{3u}	1002	w	B_{3u}
899	vw	B_{2u}	966	w	B_{3u}
875	w	B_{3u}	944	w	B_{1u}
856	s	B_{1u}	884	w	B_{3u}
809	m	B_{3u}	854	s	B_{2u}
771	w	B_{3u}	844	sh	B_{2u}
748	vw	B_{2u}	818	m	B_{3u}
645	vw	B_{2u}	802	m	B_{3u}
624	m	B_{3u}	777	w	B_{3u}
599	w	B_{3u}	753	s	B_{1u}
549	w	B_{3u}	723	w	B_{2u}
518	vw	B_{3u}	642	w	B_{2u}
497	m	B_{2u}	602	m	B_{3u}
473	s	B_{1u}	533	w	B_{3u}
			496	m	B_{2u}
			443	sh	B_{1u}
			416	s	B_{1u}
387	w				
372	vw				
294	w		292	w	
225	s		220	s	
175	w		171	w	
161	vw				
146	m		143	m	
115	s		113	s	
105	sh		103	sh	
80	w		78	w	
63	vw		58	w	

* s: strong, m: medium, w: weak, vw: very weak, sh: shoulder.

the two irreducible representations of the factor group.

Table 2 gives the normalized intensities of the vibrations belonging to the three infrared-active species B_{1u}, B_{2u}, and B_{3u} along the crystal axes a, b, and c^*, obtained from the crystal data[6] under the assumption of the oriented gas model. From Table 2, the following polarization pattern is expected from the spectra taken with polarized radiation incident perpendicularly to the ab-plane; a) the 5 fundamentals and the combinations belonging to the B_{1u} species (the out-of-plane vibrations) of the free molecule should display an exclusively greater intensity when the electric vector is parallel to the b-axis; b) the 18 fundamen-

tals and the combinations belonging to the B_{2u} and B_{3u} species (the in-plane vibrations) should instead be much stronger when the electric vector is parallel to the a-axis; c) no difference in the polarization pattern is found between the vibration bands belonging to the B_{2u} and B_{3u} species.

Figure 1 represents the polarized infrared spectra of the TCNQ and TCNQ-d_4 crystals obtained at normal incidence of radiation on the ab-plane. The solid line refers to an orientation of the electric vector parallel to the a-axis, while the broken line refers to an orientation parallel to the b-axis. The infrared data available for the TCNQ and TCNQ-d_4 crystals are collected in Table 3, together with their species determined by the discussions in this section.

It is evident from Fig. 1 that almost all the observed bands are strongly polarized when the electric vector is parallel to the a-axis, as is expected from Tables 1 and 2. The strong polarization along the b-axis is found only for one weak band at 1204 cm^{-1} and two intense bands at 856 and 473 cm^{-1} in the TCNQ spectra and one weak band at 944 cm^{-1} and two intense bands at 753 and 416 cm^{-1} in the TCNQ-d_4 spectra (indicated by arrows in Fig. 1). The two intense bands found in the respective spectra of TCNQ and TCNQ-d_4 should be identified to the B_{1u} fundamentals. Remaining three fundamentals of B_{1u} species will be found in the region less than 250 cm^{-1}. The factor group splitting expected from the correlation diagram of Table 1 is scarecely observed in Fig. 1, suggesting that the assumption of the oriented gas model holds fairly well in this case.

An attempt was made to divide the vibrations of the a-axis polarization in Fig. 1 into the B_{2u} and B_{3u} species. Inspection of Fig. 2, the schematic drawing of the b-axis projection of the molecular packing, suggests that the vibrations of the B_{3u} species give rise to stronger absorption when the polarized radiation with the electric vector parallel to the ac-plane falls upon the ab-plane at an angle of $+45°$ to the a-axis (along the x-axis), whereas the vibrations of the B_{2u} species give rise to stronger absorptions when the same polarized radiation falls upon

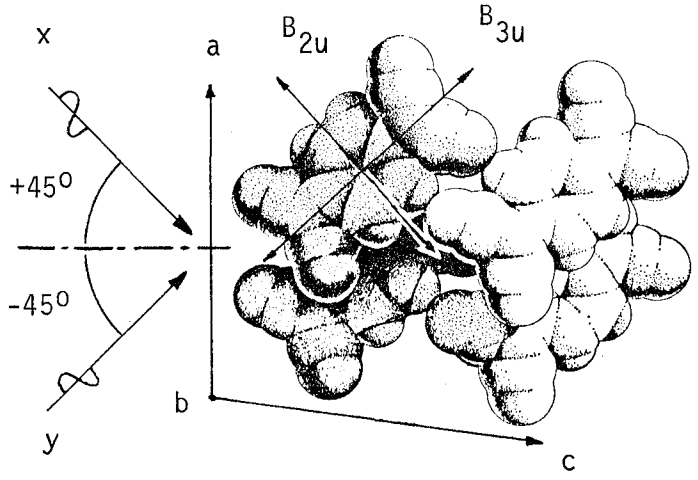

Fig. 2. Schematic drawing of the b-axis projection of the TCNQ molecules in the crystal.

the *ab*-plane at an angle of $-45°$ (along the *y*-axis). This is numerically shown in Table 4, which gives the normalized intensities of the B_{1u}, B_{2u}, and B_{3u} fundamentals along the axes *x*, *y*, and *b*, calculated from the crystal data.[6] In this case, it is difficult to decide the *x*-axis and the *y*-axis with respect to the sample plane, unless the direction of the *c*-axis is determined by the x-ray diffraction study. Table 4 indicates, however, that the absorption bands of the B_{2u} species give rise to the same polarization pattern as those of the B_{1u} species when the assumption of the oriented gas model is strictly valid.

Figure 3 represents the spectra of the TCNQ and TCNQ-d_4 crystals obtained by tilting the sample in turn by either of $\pm 45°$ (the solid and broken lines) on the *b*-axis using the polarized radiation with the electric vector parallel to the *ac*-plane. Apparently, all the absorption bands which have already been identified to the B_{1u} vibrations (indicated by arrows in Fig. 3) show the stronger absorption in the broken line spectrum than in the solid line spectrum. This fact

Table 4. Proportionality Factors for Band Intensity along *x*, *y*, and *b* Axes.

Axis	B_{1u}	B_{2u}	B_{3u}
x	0.10	0.90	0.00
y	0.06	0.01	0.93
b	0.84	0.09	0.07

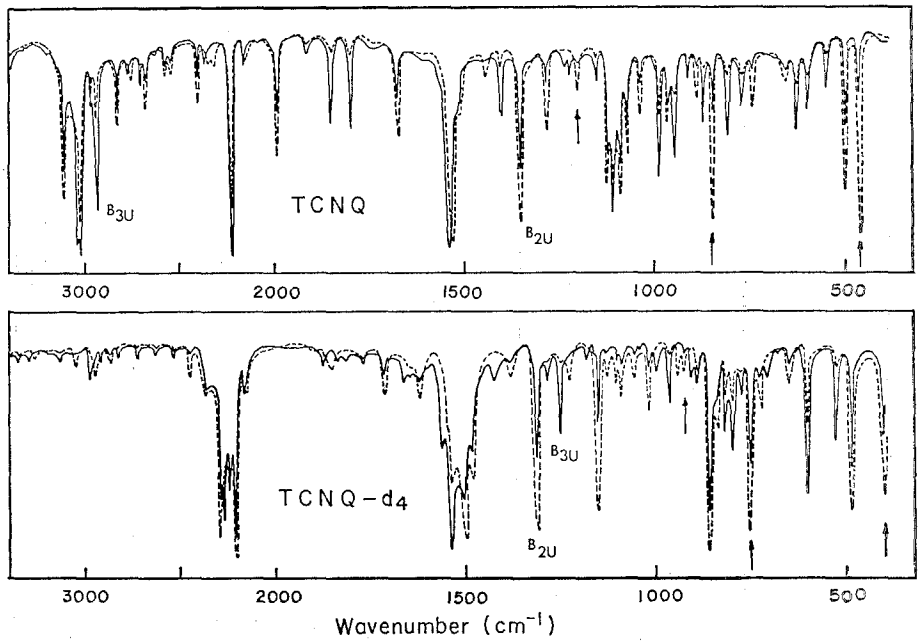

Fig. 3. Infrared spectra of TCNQ (above) and TCNQ-d_4 crystals (below) obtained by tilting the crystal plane by $\pm 45°$ on the *b*-axis and using the polarized radiation with the electric vector parallel to the *ac*-crystal plane.
——: Electric vector parallel to the *y*-axis.
– – –: Electric vector parallel to the *x*-axis (see text).

suggests that the broken line spectrum corresponds to the tilting of the sample by $-45°$ (the electric vector is parallel to the x-axis), whereas the solid line spectrum to the tilting by $+45°$ (the electric vector is parallel to the y-axis). Thus the remaining bands giving the stronger absorption in the broken line

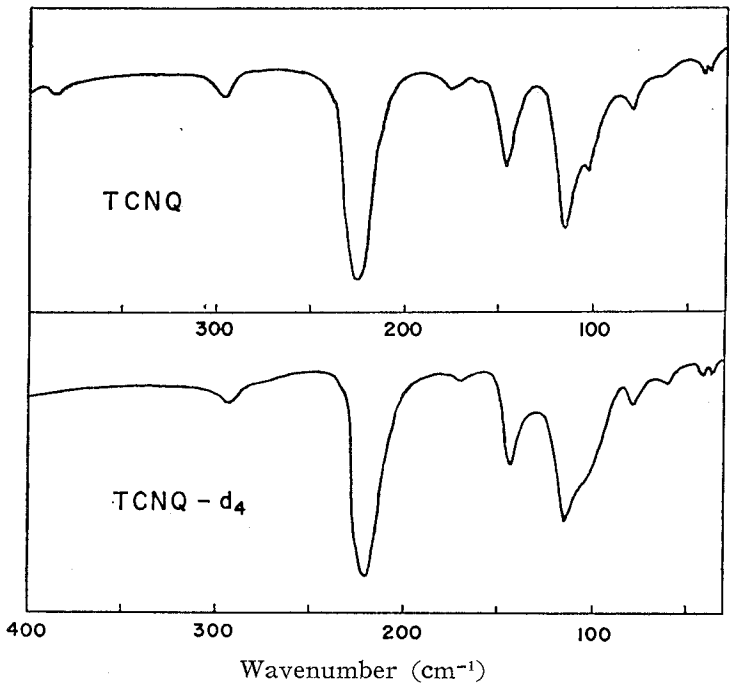

Fig. 4. Far-infrared spectra of TCNQ (above) and TCNQ-d_4 powders (below) in Nujol mulls.

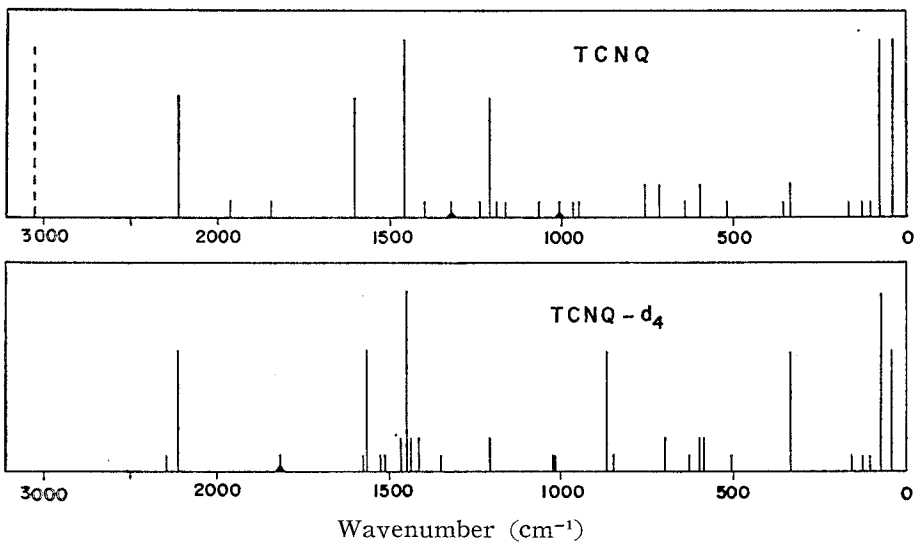

Fig. 5. Schematic drawing of Raman spectra of TCNQ (above) and TCNQ-d_4 samples (below).

spectrum are identified without ambiguity to the vibrations of the B_{2u} species and the bands giving the stronger absorption in the solid line spectrum to the vibrations of the B_{3u} species. Results are summarized in Table 3.

In Fig. 4 are shown the far-infrared spectra of TCNQ and TCNQ-4_4 powders, respectively, in Nujol mulls. Both spectra bear a close resemblance to each other. The frequencies of the observed bands are also shown in Table 3.

The Raman spectra of several lumps of TCNQ and TCNQ-d_4 crystals are schematically given in Fig. 5. The frequencies of the observed lines are collected in Table 5. Although it is difficult to experimentally classify the observed Raman lines into the respective species A_g, B_{1g}, B_{2g}, and B_{3g} because the depolarization ratios are not determined yet, the A_g fundamentals are characterized by the stronger intensity as compared with the fundamentals belonging to the other Raman-active species. The two strong Raman lines of the lowest frequencies

Table 5. Raman Spectra of TCNQ and TCNQ-d_4.

TCNQ		TCNQ-d_4	
Frequency (cm^{-1})	Intensity*	Frequency (cm^{-1})	Intensity*
——	—	2288	vw
2225	m	2225	m (b)
1960	vw	1813	vw(b)
1842	vw	1574	vw
1600	m	1564	m
1454	s	1523	vw
1398	vw	1511	vw
1319	vw(b)	1464	w
1234	vw	1448	s
1206	m	1435	w
1189	vw	1412	w
1162	vw	1348	vw
1064	vw	1204	w
1003	vw(b)	1021	vw
964	vw	1014	vw
948	vw	864	m
754	w	848	vw
713	w	695	w
638	vw	626	vw
596	w	596	w
517	vw	584	w
354	vw	503	vw
335	w	333	m
163	vw	154	vw(b)
123	vw	122	vw
103	vw	102	vw
75	s	72	s
40	s	40	m

* Symbols as in Table 3. (b) : broad.

Table 6. Fundamental Vibrations and their Assignments for TCNQ and TCNQ-d_4.

	Species	TCNQ	TCNQ-d_4	Assignment
In-plane vibration	A_g	(3071)*	2288	CH(CD) stretch.
		2225	2225	C≡N stretch.
		1600	1564	C=C stretch. (ring)
		1454	1448	C=C stretch. (side)
		1206	864	CH(CD) bend.
		1003	1014	C—C stretch. (side)
		713	695	C—C stretch. (ring)
		596	596	$C(CN)_2$ scissor.
		335	333	ring deform.
		103	102	C—C≡N bend.
	B_{1g}	(3073)*	2288	CH(CD) stretch.
		2225	2225	C≡N stretch.
		1398	1021	CH(CD) bend.
		1319	1348	C—C stretch. (ring)
		1189	1204	C—C stretch. (side)
		638	626	ring deform.
		517	503	C=$C(CN)_2$ bend.
		354	333	C—C≡N bend.
		123	122	$C(CN)_2$ rock.
	B_{2u}	3048	2295	CH(CD) stretch.
		2225	2225	C≡N stretch.
		1537	1510	C=C stretch. (ring)
		1352	1318	C—C stretch. (ring)
		1282	854	CH(CD) bend.
		1110	1160	C—C stretch. (side)
		497	496	$C(CN)_2$ rock.
		294	292	C—C≡N bend.
		80	78	C=$C(CN)_2$ bend.
	B_{3u}	3062	2283	CH(CD) stretch.
		2225	2225	C≡N stretch.
		1543	1531	C=C stretch. (side)
		1402	1249	CH(CD) bend.
		996	966	C—C stretch. (side)
		960	802	C—C stretch. (ring)
		624	602	$C(CN)_2$ scissor.
		549	533	ring deform.
		146	143	C—C≡N bend.
Out-of-plane vibration	B_{1u}	856	753	CH(CD) bend.
		473	416	$C(CN)_2$ wag.
		225	220	C=$C(CN)_2$ bend.
		175	171	C—C≡N bend.
		115	113	ring deform.
	B_{2g}	948	848	CH(CD) bend.
		163	154	C—C≡N bend.
	B_{3g}	754	584	CH(CD) bend.
		163	154	C—C≡N bend.

* ( ): Calculated value, see text.

observed in the respective spectra (75 and 40 cm^{-1} for TCNQ and 72 and 40 cm^{-1} for TCNQ-d_4) should be attributed to a part of the lattice vibrations due to the molecular rotation.*

IV. VIBRATIONAL ASSIGNMENT

In order to make assignment of the observed frequencies to the fundamental modes, the following examinations were carried out besides the discussions in the previous section; a) comparison of the spectral data with those of partly analogous molecules such as TCNE[1,7,8] and *p*-benzoquinone and its deuterated derivatives[9]; b) application of the product rule[2,3] and the modified sum rule[4] for the TCNQ and TCNQ-d_4 fundamentals; c) the normal coordinate analysis of the in-plane vibrations of the TCNQ and TCNQ-d_4 molecules.

The observed frequencies thus determined as the fundamentals are listed for the TCNQ and TCNQ-d_4 molecules in Table 6, together with their vibrational assignments. Since the Raman lines of the TCNQ molecule around 3000 cm^{-1}, which are assigned to the CH stretching modes of the A_g and B_{1g} species, have not been recorded as is described before, the calculated values are given in parentheses in Table 6. Furthermore, some of the Raman lines assignable to the B_{2g} and B_{3g} fundamentals (the out-of-plane vibrations) have not yet been observed. Table 7 shows the results obtained by applying the product rule[2,3] and the modified sum rule[4] to the TCNQ and TCNQ-d_4 fundamentals. On the product rule, a good agreement of $\prod_k [\nu_k(\text{TCNQ-d}_4)/\nu_k(\text{TCNQ})]$ was found between the theoretical and the experimental values for all but the B_{2g} and B_{3g} species just mentioned. On the modified sum rule, on the other hand, a good agreement of $[\sum_k \lambda_k(\text{TCNQ}) - \sum_k \lambda_k(\text{TCNQ-d}_4)]$ was obtained among all the in-plane species.

Table 7. Results of Applying the Product Rule and Modified Sum Rule for TCNQ and TCNQ-d_4 Fundamentals.

Product rule

	A_g	B_{1g}	B_{2g}	B_{3g}	B_{1u}	B_{2u}	B_{3u}
Theoretical	0.500	0.501	0.710	0.716	0.714	0.505	0.505
Experimental	0.504	0.501	——	——	0.726	0.485	0.490

Modified sum rule for in-plane species

A_g	B_{1g}	B_{2u}	B_{3u}
2.97	2.98	2.95	2.94

* According to the factor group analysis for the Bravais unit cell of the TCNQ crystal, there are nine lattice vibrations. Of these vibrations the three are the Raman-active modes of the A_g species, the three are the Raman-active modes of the B_g species, the two are the infrared-active modes of the A_u species, and the remaining one is the infrared-active mode of the B_u species. The Raman-active lattice modes are due to the molecular rotation and are said to give strong lines. The infrared-active modes are due to the molecular translation.

Table 8. Assignments of Observed Infrared Bands and Raman Lines due to Overtone and Combination Vibrations.

	TCNQ				TCNQ-d_4			
	Frequency (cm^{-1})	Intensity	Species experimentally determined	Assignment	Frequency (cm^{-1})	Intensity	Species experimentally determined	Assignment
Raman line	1960	vw		$1319(B_{1g})+638(B_{1g})=1957(A_g)$	Raman line	1813	vw		$1318(B_{2u})+496(B_{2u})=1814(A_g)$
				$996(B_{3u})+960(B_{3u})=1956(A_g)$		1574	vw		$1160(B_{2u})+416(B_{1u})=1576(B_{3g})$
	1842	vw		$1352(B_{2u})+497(B_{2u})=1849(A_g)$					$966(B_{3u})+602(B_{3u})=1568(A_g)$
				$1319(B_{1g})+517(B_{1g})=1836(A_g)$		1523	vw		$2225(A_g)-695(A_g)=1530(A_g)$
	1234	vw		$624(B_{3u})\times2=1248(A_g)$		1511	vw		$753(B_{1u})\times2=1506(A_g)$
				$2225(B_{3u})-996(B_{3u})=1229(A_g)$		1464	w		$1564(A_g)-102(A_g)=1462(A_g)$
				$1537(B_{2u})-294(B_{2u})=1243(A_g)$					$1348(B_{1g})+122(B_{1g})=1470(A_g)$
	1162	vw		$638(B_{1g})+517(B_{1g})=1155(A_g)$					$864(A_g)+596(A_g)=1460(A_g)$
				$624(B_{3u})+549(B_{3u})=1173(A_g)$		1435	w		$2295(B_{2u})-854(B_{2u})=1441(A_g)$
	1064	vw		$1189(B_{1g})-123(B_{1g})=1066(A_g)$					$1510(B_{2u})-78(B_{2u})=1432(A_g)$
				$1352(B_{2u})-294(B_{2u})=1058(A_g)$					$848(B_{2g})+584(B_{3g})=1432(B_{1g})$
	964	vw		$1319(B_{1g})-354(B_{1g})=965(A_g)$		1412	w		$802(B_{3u})=602(B_{3u})=1404(A_g)$
				$856(B_{1u})+115(B_{1u})=971(A_g)$					
Infrared band	3135	m	B_{2u}	$1600(A_g)+1537(B_{2u})=3137(B_{2u})$	Infrared band	2965	w	B_{3u}	$2283(B_{3u})+695(A_g)=2978(B_{3u})$
	2970	m	B_{3u}	$3062(B_{3u})-103(A_g)=2959(B_{3u})$		2943	w	B_{2u}	$1510(B_{2u})+1448(A_g)=2958(B_{2u})$
	2848	w	B_{2u}	$2225(B_{1g})+624(B_{3u})=2849(B_{2u})$		2420	w	B_{2u}	$1564(A_g)+854(B_{2u})=2418(B_{2u})$
	2710	w	B_{2u}	$1600(A_g)+1110(B_{2u})=2710(B_{2u})$		2262	m	B_{3u}	$1249(B_{3u})+1014(A_g)=2263(B_{3u})$
				$1402(B_{3u})+1319(B_{1g})=2721(B_{2u})$		2175	w	B_{3u}	$2295(B_{2u})-122(B_{1g})=2173(B_{3u})$
	2412	w	B_{2u}	$3062(B_{3u})-638(B_{1g})=2424(B_{2u})$					$1160(B_{2u})+1021(B_{1g})=2181(B_{3u})$
	1995	m	B_{2u}	$1282(B_{2u})+713(A_g)=1995(B_{2u})$		1839	w	B_{2u}	$1510(B_{2u})+333(A_g)=1843(B_{2u})$
	1858	m	B_{3u}	$3062(B_{3u})-1206(A_g)=1856(B_{3u})$		1722	m	B_{2u}	$2225(A_g)-496(B_{2u})=1729(B_{2u})$
				$3048(B_{2u})-1189(B_{1g})=1859(B_{3u})$					$864(A_g)+854(B_{2u})=1718(B_{2u})$
	1804	m	B_{3u}	$1319(B_{1g})+497(B_{2u})=1816(B_{3u})$		1628	m	B_{2u}	$2225(B_{2u})-596(A_g)=1629(B_{2u})$
				$1282(B_{2u})+517(B_{1g})=1799(B_{3u})$					$1021(B_{1g})+602(B_{3u})=1623(B_{2u})$

1668	m	B_{2u}	$1543(B_{3u})+123(B_{1g})=1666(B_{2u})$	1555	w	B_{3u}	$1014(A_g)+533(B_{3u})=1547(B_{3u})$
			$3062(B_{3u})-1398(B_{1g})=1664(B_{2u})$				$966(B_{3u})+596(A_g)=1562(B_{3u})$
			$2225(B_{1g})-549(B_{3u})=1676(B_{2u})$	1495	m	B_{2u}	$1348(B_{1g})+143(B_{3u})=1491(B_{2u})$
1204	w	B_{1u}	$856(B_{1u})+335(A_g)=1191(B_{1u})$				$1160(B_{2u})+333(A_g)=1493(B_{2u})$
1122	m	B_{3u}	$948(B_{2g})+175(B_{1u})=1123(B_{3u})$	1435	m	B_{3u}	$2288(B_{1g})-854(B_{2u})=1434(B_{3u})$
			$2225(B_{1g})-1110(B_{2u})=1115(B_{3u})$				$1318(B_{2u})+122(B_{1g})=1440(B_{3u})$
1089	m	B_{2u}	$596(A_g)+497(B_{2u})=1093(B_{2u})$	1395	m	B_{2u}	$1510(B_{2u})-102(A_g)=1408(B_{2u})$
1042	w	B_{2u}	$2225(B_{3u})-1189(B_{1g})=1036(B_{2u})$	1234	w	B_{2u}	$626(B_{1g})+602(B_{3u})=1228(B_{2u})$
			$1402(B_{3u})-354(B_{1g})=1048(B_{2u})$	1128	w	B_{2u}	$2288(A_g)-1160(B_{2u})=1128(B_{2u})$
			$1189(B_{1g})-146(B_{3u})=1043(B_{2u})$				$802(B_{3u})+333(B_{1g})=1135(B_{2u})$
875	w	B_{3u}	$549(B_{3u})+335(A_g)=884(B_{3u})$	1090	m	B_{2u}	$1014(A_g)+78(B_{2u})=1092(B_{2u})$
809	m	B_{3u}	$3048(B_{2u})-2225(B_{1g})=823(B_{3u})$				$966(B_{3u})+122(B_{1g})=1088(B_{2u})$
			$1402(B_{3u})-596(A_g)=806(B_{3u})$				$596(A_g)+496(B_{2u})=1092(B_{2u})$
			$517(B_{1g})+294(B_{2u})=811(B_{3u})$	1054	w	B_{2u}	$1160(B_{2u})-102(A_g)=1058(B_{2u})$
771	w	B_{3u}	$2225(B_{3u})-1454(A_g)=771(B_{3u})$	1019	m	B_{2u}	$2225(B_{3u})-1204(B_{1g})=1021(B_{2u})$
			$1282(B_{2u})-517(B_{1g})=765(B_{3u})$	944	w	B_{1u}	$1510(B_{2u})-584(B_{3g})=926(B_{1u})$
			$948(B_{2g})-175(B_{1u})=773(B_{3u})$	884	w	B_{3u}	$1510(B_{2u})-626(B_{1g})=884(B_{3u})$
599	w	B_{3u}	$1600(A_g)-996(B_{3u})=604(B_{3u})$	818	m	B_{3u}	$1318(B_{2u})-503(B_{1g})=815(B_{3u})$
			$1110(B_{2u})-517(B_{1g})=593(B_{3u})$	777	w	B_{3u}	$2288(B_{1g})-1510(B_{2u})=778(B_{3u})$
			$517(B_{1g})+80(B_{2u})=597(B_{3u})$				$2225(B_{3u})-1448(A_g)=777(B_{3u})$
				723	w	B_{2u}	$1318(B_{2u})-596(A_g)=722(B_{2u})$
							$1014(A_g)-292(B_{2u})=722(B_{2u})$
							$602(B_{3u})+122(B_{1g})=724(B_{2u})$
				642	w	B_{2u}	$503(B_{1g})+143(B_{3u})=646(B_{2u})$

Here λ_k is the frequency parameter of the kth fundamental vibration and is related with its frequency ν_k (cm^{-1}) by

$$\lambda_k = 4\pi^2 c^2 \nu_k^2.$$

The normal coordinate treatments for the in-plane vibrations were carried out using the Urey-Bradley force field.[10,11] The agreement between the calculated and the observed frequencies was satisfactory except for a few fundamentals. An attempt to have a better agreement is being made using the modified Urey-Bradley force field which contains some interaction terms between the various internal coordinates of the molecule. A detail of the calculation will be reported elsewhere.

Besides the infrared bands and the Raman lines assigned to the fundamental vibrations, there remain a number of frequencies attributable to the overtone or combination vibrations. According to the selection rule, these Raman lines and infrared bands were assigned as is shown in Table 8. It may be noticed that almost all the Raman lines are associated with the A_g mode. Since all the A_u frequencies and some of the B_{2g} and B_{3g} frequencies have not yet been established, the overtones and combinations involving those vibrations were not considered. Nevertheless, for each of the observed frequencies, one or more possible assignments were found, and the agreement between the calculated and observed values is satisfactory as Table 8 shows.

ACKNOWLEDGMENTS

The author wishes to express his gratitude to Professor Emeritus Rempei Gotoh for his continuing interest and encouragement during the course of this work. Thanks are also due to Dr. Natsu Uyeda of this institute for supplying the TCNQ sample, to Dr. Shinzaburo Oka of this institute for synthesizing the TCNQ-d_4 sample, to Dr. Mitsuo Ito of the University of Tokyo for measuring the laser Raman spectra of the TCNQ and TCNQ-d_4 crystals, and to Dr. Soichi Hayashi of this institute for his valuable discussions.

REFERENCES

(1) T. Takenaka and S. Hayashi, *Bull. Chem. Soc. Japan*, 37, 1216 (1964).
(2) O. Redlich, *Z. phys. Chem.*, (B), 28, 371 (1935).
(3) E. Teller (quoted by C. K. Ingold *et al.*), *J. Chem. Soc.*, 1936, 971.
(4) K. Machida, *J. Chem. Phys.*, 38, 1360 (1963).
(5) D. S. Acker and W. R. Hertler, *J. Am. Chem. Soc.*, 84, 3370 (1962).
(6) R. E. Long, R. A. Sparks, and K. N. Trueblood, *Acta Crys.*, 18, 932 (1965).
(7) F. A. Miller *et al.*, *Spectrochim. Acta*, 20, 1233 (1964).
(8) A. Rosenberg and J. P. Devlin, *ibid.*, 21, 1613 (1965).
(9) E. D. Becker, E. Charney, and T. Anno, *J. Chem. Phys.*, 42, 942 (1965).
(10) H. C. Urey and C. A. Bradley, *Phys. Rev.*, 38, 1969 (1931).
(11) T. Shimanouchi, *J. Chem. Phys.*, 17, 245, 734, 848 (1949).